Numerical simulation of localized impedance along a segmented PEM fuel cell

S. CHEVALIER[a,b,*] , C. JOSSET[b], JC OLIVIER[a], B. AUVITY[b], D. TRICHET[a], M. MACHMOUM[a]

[a] IREENA, University of Nantes, Saint Nazaire, France

[b] Laboratoire de Thermocinétique de Nantes (CNRS UMR 6607), Polytech Nantes, France

* stephane.chevalier@univ-nantes.fr

ABSTRACT

A pseudo 2D PEM fuel cell model is developed. Based on fundamentals phenomena, a.c. and d.c. modelling are presented showing that the gas oscillation through the channels can be numerically reproduced along a segmented cell. Numerical results are then compared to experimental cell impedances under different air stoichiometry conditions. Model inversion is done thanks to an hybrid criterion, based on cell impedance as well as d.c. current. Good agreement between the model and cell measurements are obtained, the general stoichiometry effect is numerically reproduced and the gas channel oscillations impact on impedance measurements is quantified. The results shows that wrong evaluation of oxygen diffusion coefficient may be obtained if this effect is neglected, as it generally done with classical 1D physical model.

1. INTRODUCTION

Nowadays, PEM fuel cell performances are generally evaluated using electrochemical methods as impedance spectroscopy [1]. Coupled with numerical models, fuel cell main characteristics as electrode platinum loading, membrane resistance, gas transport properties, may be extracted. Different models are reported through the literature, the so-called Randles circuit [2] is among the most common to fit fuel cell impedances. Recent papers have shown its suitability as a diagnostic tool [3, 4]. More complex cell impedance model have been proposed by Springer et al. and Eikerling and Kornyshev [5, 6] and at the end of the nineties. They are based on the electrochemical equations occurring through the membrane electrode assembly (MEA). Although, numerically heavier than the electrical equivalent circuit models, they offer more information concerning the cell intrinsic parameters and they are also able to reproduced cell a.c. behaviour over a large range of operating voltages [7].

Recent experimental results reported by Schneider et al. [8] have recently shown gas oscillations through the cathode channel. This effect may have a non neglected impact on the cell impedance. Then, this experimental observations are confirmed by Kulikovsky [9] and Maranzana et al. works, [10]. Based on pseudo 2D models, they were able to reproduced the gas oscillations through the channels. Nevertheless, to the authors knowledge, no experimental validations have been done. Indeed, although Maranzana et al. have proposed a dimensionless number to estimate this effect, its quantification on classical cell configuration has not been done.

Thus, in this paper we report experimental impedance results of commercial cells with parallel channels. The pseudo 2D model used is presented in section 2, and then fitted on our experimental data, section 3. In the final part, we discuss about the gas oscillations impact over the total cell measured impedance.

2. D.C. AND A.C. FUEL CELL MODELLING

2.1 Fuel cell geometry

The studied cell is based on the commercials cells developed by Swiss society MES DEA. These are particular suited to run under low temperatures and ambient pressure. To reduce the pressure drop along cathode channels, the bipolar plates are constituted of several parallel channels, that ensure less pressure drop than the classical serpentine configuration. Air is then distributed through the gas diffusion layer and then reaches the membrane electrode assembly (MEA) as schemed on Figure 2 below. This particular geometry is well suited to pseudo 2D models as theses developed by [9] and [10]. It is based on the assumption that the

cell current densities flow only on the *x* direction. Finally, knowing the consumed molar oxygen flux by each MEA slices, the molar concentration distribution may be computed through the channel, see Figure 2.

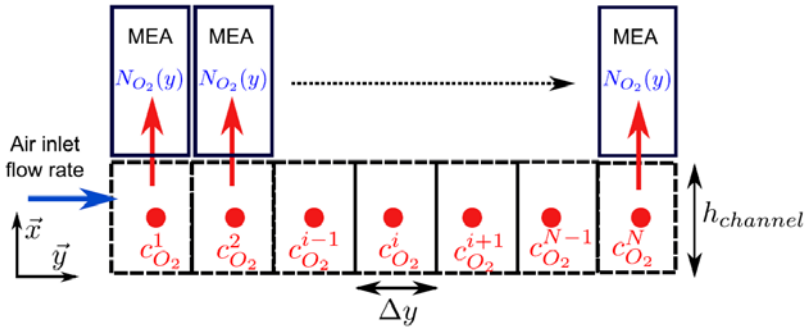

Figure 1. Pseudo 2D fuel cell model

2.2 Generals equations

As depicted on Figure 2, ionic and oxygen transport are described through the membrane, electrode and GDL. Only cathode electrochemical transfers are modelled, anode is assumed as being no limiting through the cells reactions. Thus, its impedance may also be neglected.

Concerning the water produced by the fuel cell oxygen and hydrogen reaction, its impact is not modelled here, but its role on cell performances may be seen through the cell intrinsic properties like the membrane resistance, GDL gas diffusion coefficients, exchange currents... Increasing or decreasing these properties may be linked to a cell state of health [3].

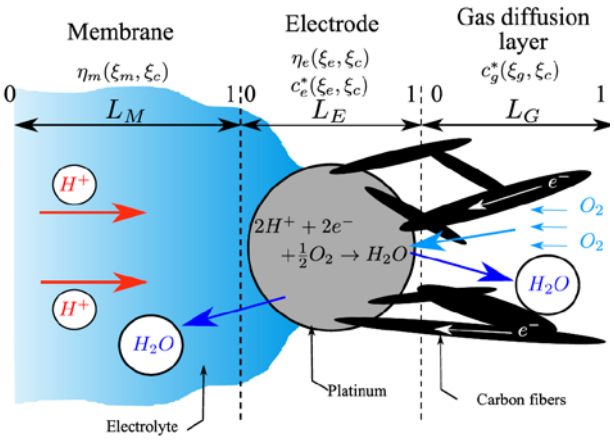

Figure 2. Scheme of the electrochemical process intrinsic to the PEM fuel cell. The model variables are pointed out each domains where they are solved.

The general fuel cells equations are based on Ohm's law, Fick's law, Tafel's law and the charge and mass conservations. Through the three domains depicted on Figure 2, the electrochemical transfers are described by the equations below. In the following model, electronic transport through the GDL is neglected, thus cell voltage may be obtained directly by computing the overpotential.

$$-\sigma_m \frac{d^2\eta_m}{dx_m^2} = 0 \quad (1)$$

$$-\sigma_e \frac{\partial^2\eta_e}{\partial x_e^2} + \frac{C_{DL}}{L_e}\frac{\partial\eta_e}{\partial t} = -A_r i_c \frac{c_e}{c^{ref}} \exp\left(\frac{\eta_e}{b}\right) \quad (2)$$

$$-D_e \frac{\partial^2 c_e}{\partial x_e^2} + \frac{\partial c_e}{\partial t} = -\frac{A_r i_c}{4.F}\frac{c_e}{c^{ref}} \exp\left(\frac{\eta_e}{b}\right) \quad (3)$$

$$-D_g \frac{\partial^2 c_g}{\partial x_g^2} + \frac{\partial c_g}{\partial t} = 0 \quad (4)$$

This system is solved on each abscise *y*. The oxygen concentration through the channels is governed only by advection, it can be written as:

$$\frac{\partial c_c}{\partial t} + u_c \frac{\partial c_c}{\partial y} = -\frac{N_{O_2}(y)}{h_{channel}}\Big|_y \quad (5)$$

Where N_{O_2} is the oxygen molar flux entering through the GDL at abscise *y* and u_c the air velocity through one channel. The previous five equations are solved first in steady regime to obtain the cell working point, then in periodic regime at several frequencies to compute the cell impedance along the channel.

2.3 Steady states model

To simplify the computation, let us define the following variables:

- Respectively the channel, GDL and electrode dimensionless coordinates : $\xi_c = \frac{y}{L_c}$, $\xi_g = \frac{x}{L_g}$ and $\xi_e = \frac{x}{L_e}$
- Respectively the channel, GDL and electrode dimensionless molar concentrations: $c_c^* = \frac{c_c}{c^{ref}}$, $c_g^* = \frac{c_g}{c^{ref}}$ and $c_e^* = \frac{c_e}{c^{ref}}$
- The charge transfer coefficient: $\kappa = \frac{A_r.i_c.{L_e}^2}{\sigma_e}$
- The mass transfer coefficient: $\gamma = \frac{A_r.i_c.{L_e}^2}{4.F.D_e.c^{ref}}$
- Respectively the GDL and membrane shape factor: $\lambda_g = \frac{L_g.D_e}{L_e.D_g}$ and $\lambda_m = \frac{L_m.\sigma_e}{L_e.\sigma_m}$
- The membrane resistance: $R_m = \frac{\sigma_m}{L_m}$
- The channel transport coefficient: $\mu = \frac{L_c.D_g}{h_c.u_c.L_g}$

Equations (1) and (4) are solved analytically in steady state, with the previous notation, the membrane overpotential and GDL molar concentration are written as:

$$\eta_m^0 = \left(\eta_e^0(0) - E^{ref} + E_{cell}\right).\xi_m + E^{ref} - E_{cell} \quad (6)$$

$$c_g^* = (c_c^*(\xi_c) - c_e^*(1)).\xi_m + c_e^*(1) \quad (7)$$

With E^{ref} the so-called reference potential, i.e. 1.23 V, E_{cell} the cell potential and $c_c^*(\xi_c)$ the channel oxygen concentration at the abscise ξ_c. Both previous equations are dependant of the electrode electrochemical transfers through the two coefficients $\eta_e^0(0)$ and $c_e^*(1)$. They are obtained by numerically solving the following system. The boundary conditions (equations 10 to 13) are computed from the ionic and mass flux conservation on each electrode boundary, see Figure 2.

$$\frac{d^2{\eta_e}^0}{d{\xi_e}^2} = \kappa.c_e^*.\exp\left(\frac{{\eta_e}^0}{b}\right) \quad (8)$$

$$\frac{d^2c_e^*}{d{\xi_e}^2} = \gamma.c_e^*.\exp\left(\frac{{\eta_e}^0}{b}\right) \quad (9)$$

$$\frac{d\eta_e}{d\xi_e}\Big|_0 = \frac{1}{\lambda_m}\frac{d\eta_m}{d\xi_m}\Big|_1 = -\frac{\eta_e^0(0) - E^{ref} + E_{cell}}{\lambda_m} \quad (10)$$

$$\frac{d\eta_e}{d\xi_e}\Big|_1 = 0 \quad (11)$$

$$\frac{dc_e^*}{d\xi_e}\Big|_0 = 0 \quad (12)$$

$$\frac{dc_e^*}{d\xi_e}\Big|_1 = \frac{1}{\lambda_g}\frac{d\eta_g}{d\xi_g}\Big|_0 = \frac{c_c^*(\xi_c) - c_e^*(1)}{\lambda_g} \quad (13)$$

The coupled equations 8 and 9 are solved using the finite volume method on 30 nodes, that ensure mesh convergence. Then, the oxygen molar flux consumed is deduced to compute the concentration distribution through the channel. Still using the previous developed notations, the steady channel concentration is written:

$$\frac{dc_c^*}{d\xi_c} = \mu.(c_c^* - c_e^*(1)) \quad (14)$$

Equation 14 is solved using backward finite difference scheme: firstly electrochemical transfers are solve on mesh *i*, secondly using equation 14, the new oxygen channel concentration is computed on mesh *i+1*, and MEA transfer are again solved. Thus, the local current densities distribution along the channel are obtained. The cell current is finally computed by:

$$j_{cell} = \int_0^1 \frac{\left(\eta_e^0(0,\xi_c) - E^{ref} + E_{cell}\right)}{R_m} . d\xi_c \quad (15)$$

2.4 Harmonic model

Equations 1 to 4 are now transformed through frequency domain by decomposing each field into a steady and a periodic part, i.e. : $\eta_e(x,t) = {\eta_e}^0(x) + \delta\eta_e(x,\omega).\exp(i.\omega.t)$. This assumption is remain true while the complex variation is $\delta\eta_e(x,\omega) \ll 1$, that can be posteriori check. Three characteristic angular frequencies are also introduced:

- $\omega_e = \frac{\sigma_e}{C_{DL}.L_e}$ linked to charge transfers
- $\omega_g = \frac{D}{{L_g}^2}$ linked to gas diffusion through the GDL
- $\omega_c = \frac{u_c}{L_c}$ linked to the gas transport through the channel.

As previously, the equations 1 and 4 have been solved analytically in periodic state. The complex membrane overpotential and oxygen molar concentration are written as:

$$\delta\eta_m = -R_m.\delta j(\xi_m - 1) + \delta\eta_e(0) \quad (16)$$

$$\delta c_g^* = \delta c_e^*(1).\cosh\left(\sqrt{\frac{i.\omega}{\omega_g}}.\xi_g\right) + \left(\frac{\delta c_c^*(\xi_c)}{\sinh\left(\sqrt{\frac{i.\omega}{\omega_g}}\right)} - \coth\left(\sqrt{\frac{i.\omega}{\omega_g}}\right).\delta c_e^*(1)\right).\sinh\left(\sqrt{\frac{i.\omega}{\omega_g}}.\xi_g\right) \quad (17)$$

Where $i = \sqrt{-1}$ is the complex number, ω the angular frequency and δj the amplitude of the exciting current taken to 10% of DC current. Then, the periodic electrochemical transfer in the electrode are described by the following set of equations:

$$\frac{d^2\,\delta\eta_e}{d{\xi_e}^2} = \kappa.\exp\left(\frac{{\eta_e}^0}{b}\right).\left(c_e^{*0}\frac{\delta\eta_e}{b} + \delta c_e^*\right) + i.\frac{\omega}{\omega_e}\delta\eta_e \quad (18)$$

$$\frac{d^2\,\delta c_e^*}{d{\xi_e}^2} = \gamma.\exp\left(\frac{{\eta_e}^0}{b}\right).\left(c_e^{*0}\frac{\delta\eta_e}{b} + \delta c_e^*\right) + i.\frac{\omega}{{\lambda_g}^2.\omega_g}\delta c_e^* \quad (19)$$

$$\left.\frac{d\,\delta\eta_e}{d\xi_e}\right|_0 = -\frac{R_m.\delta j}{\lambda_m} \quad (20)$$

$$\left.\frac{d\,\delta\eta_e}{d\xi_e}\right|_1 = 0 \quad (21)$$

$$\left.\frac{d\,\delta c_e^*}{d\xi_e}\right|_0 = 0 \quad (22)$$

$$\left.\frac{d\,\delta c_e^*}{d\xi_e}\right|_1 = -\frac{\sqrt{i.\frac{\omega}{\omega_g}}}{\lambda_g}\left(\frac{\delta c_c^*(\xi_c)}{\sinh\left(\sqrt{i.\frac{\omega}{\omega_g}}\right)} - \coth\left(\sqrt{i.\frac{\omega}{\omega_g}}\right).\delta c_e^*(1)\right) \quad (23)$$

Finally the distribution of periodic oxygen concentration is also computed through the channels, it is described by:

$$\frac{d\,\delta c_c^*}{d\xi_c} = \mu.\left.\frac{d\,\delta c_g^*}{d\xi_g}\right|_1 - i.\frac{\omega}{\omega_c}\delta c_c^* \quad (24)$$

Once the perturbed overpotential is known through the membrane, it is possible to compute the cell global impedance as:

$$\frac{1}{Z_{cell}} = \int_0^1 \frac{\delta j}{\delta\eta_m(0,\xi_c)} . d\xi_c \quad (25)$$

3. EXPERIMENTAL VALIDATION

3.1 Fuel cell impedance measurements

In order to obtain intrinsic fuel parameters like, i.e. Tafel slope, oxygen diffusion coefficient..., experimental fuel cell impedance measurements are carried out. A sixteen cells stack is connected to a conditioning gas

bench (air and hydrogen) where reactants flow rate, temperature, hygrometry and pressures are monitored. Moreover, a 1.5kW electronic load is used to measure stack performances. Note that every single cell voltage is recorded and their impedance may be measured thanks to 16 parallel frequency response analysers purchased by the company Material Mates [11]. Although the model may be fitted on every cell impedance, only one cell response is used in the following results: the cell number 5 which is representative of the general cell behaviour.

In this following sample, the operating current have been set to 30 A (0.5 A/cm²) and air stoichiometry have been successively set from 10, 5, 4 and 3. The others experimental parameters are summarised in the Table 1. The measurements have been carried out based on this home-made protocol: the stack is stabilised during 600 seconds, then two spectroscopy are successively run from 1 kHz to 10 mHz with 6A modulation. The value of 20% of DC current has been preferred rather than 10% to enhance the cell response sensitivity.

Table 1.Fuel cell experimental conditions

Parameters	Value
Hydrogen Stoichiometry	2.0
Hydrogen relative humidity (%)	0
Air relative humidity (%)	0
Stack Temperature (°C)	40

3.2 Model inversion and identified parameters

All the model parameters are summarised through the Table 2. Among them, six parameters are fitted on experimental cell impedances, see physical properties on Table 2, the obtained value are the literature range. Previous results [5, 7] have shown that several operating point are needed to obtain enough sensitivity on each parameters. Highest electrochemists parameters sensitivities are obtained on high cell voltages whereas diffusion parameters should be obtained on low cell voltages. Nevertheless, 30 A may be considered as an intermediate point (between high and low voltages) where all parameters are enough sensitive and well uncorrelated.

On other hand, steady current densities and overpotential are computed by our model as well as the cell harmonic response on several frequencies. Thus, this two data may be used to correctly fit the model on experimental data, an hybrid criterion χ is thus developed based on the a.c. (Z_{exp}) and d.c. (I_{exp}) cell measurements:

$$\chi = \sum_n \left\| Z_{model}\left(\omega^n\right) - Z_{exp}\left(\omega^n\right) \right\|^2 + \Theta . \left\| I_{model} - I_{exp} \right\|^2 \quad (26)$$

The parameter Θ is used to regulate the global criterion, it has been empirically set to 10^{-7} that ensure an equilibrium between both cell impedance and current criteria. This allow a model fitting on the cell impedance measurement as well as the cell polarisation curve. Model inversion is then carried out by a simplex algorithm on Matlab®, through the subroutine *fminsearch*.

Table 2.Model parameters

Geometrie	Value	Physical properties	Value
Channels length (mm) L_c	144	Tafel Slope (V) b	0.074
Channel height (mm) h_c	1	Volumetric exchange current (A/m^3) $A_r . i_c$	6.32 10^5
Channel section (mm²) S_c	2	Oxygen Diffusivity (m^2/s) D_o	7.03 10^{-6}
Membrane thickness (mm) L_g	MCD[1]	Membrane conductivity (S/m) σ_m	2.23
GDL thickness (mm) L_g	MCD[1]	Double layer capacity (F/m^2) C_{DL}	176.12
Electrode thickness (mm) L_e	MCD[1]	Reference concentration (mol/m^3) c^{ref}	2.12

3.3 Results

The figure below summarised the experimental results and model fitting based on the previous parameters set. As it is generally admitted, cell impedance generally shows two distinct loops in Nyquist plot: kinetic

[1] MCD: Manufacturer confidential data.

and diffusive loop on respectively high and low frequency. But a third loop on lower frequencies can be also seen, as shown by Schneider et al. [8], it is the so-called channel impedance due to the gas oscillation through the channels. On the reported measurements here, at least this both loops, i.e. kinetic and diffusion, may be pointed out.

Numerical results presented on Figure 3 shows good agreements with experimental data. The global cell behaviour is well reproduced: low frequencies loop grows as air stoichiometry decreases. The four numerical impedances have been computed using the same parameters set, only the inlet stoichiometry is modified. The deviation seen on higher frequency can be attributed to water accumulation through the membrane electrode assembly, particularly on low stoichiometry conditions. Water tends to decrease the cell exchange current that increase its impedance through this frequency range. Moreover, the model is also able to predict the right frequency range (Figure 3(b)) as well as the right operating current, see Table 3.

Table 3. Numerical results. The experimental operating current was set to 30 A.

Air Stoichiometry	**Operating Voltages (measured)**	**Operating currents (computed)**
10	0.658 V	31.32 A
5	0.658 V	31.05 A
4	0.655 V	30 .56 A
3	0.638 V	31. 82 A

(a) (b)

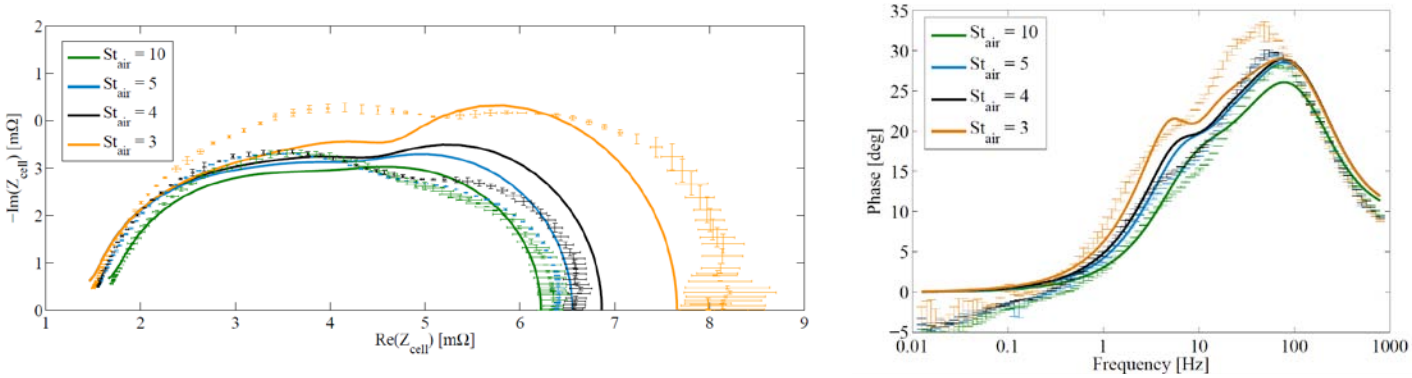

Figure 3. Cell impedance results. Model is plotted with solid line and experimental data with dot, error bars show the standard deviation. (a) Nyquist plot, (b) Bode plot.

4. IMPEDANCE ANALYSIS

4.1 Gas channel impedance

As it is generally admitted, gas oscillations may appear under relative low stoichiometry conditions through parallel channel that is the experimental conditions reported herein. Thus, the previous numerical model may be used to estimate the channel impedance impact. Figure 4.a shows the local impedances reported along the gas channel with air stoichiometry of 3. Although, only two loops are obtained at the inlet, the third channel loop clearly appears as gases reach the outlet. Comparison with impedance obtained without gas oscillations is done: the same model is solved with gas channel perturbation δc_c^* set to zero along the entire channel. In this case, no channel loop can be pointed out. Even if the local impedances grow along the channel, this effect is only linked to the oxygen depletion. The deviation with the total impedance clearly shows the non negligible channel impedance effect, particularly close to the outlet. This result are in agreement with the theoretical development of Kulikovsky and Maranzana et al. [9, 10].

On other hand, gas oscillations characteristic frequencies may be extracted from the model. Figure 4.b shows the modulus of the gas channel perturbations computed at different frequency. As expected, gas oscillations are maximum close to outlet. This maximum is also obtained around 1-5 Hz, that is close to the characteristic

frequency: $f_c = 2.\pi.\omega_c \approx 2$ Hz. These is in the range usually recorded. Moreover, the diffusion characteristic frequency obtained is also is this same range (5.5 Hz), explaining why this third loop is not clearly visible on experimental data. Both phenomena occurring in the same frequency, that means 1D model may wrongly link the low frequency loop exclusively to gas diffusion effect through the GDL. An example is illustrated in the next final section.

(a) (b)

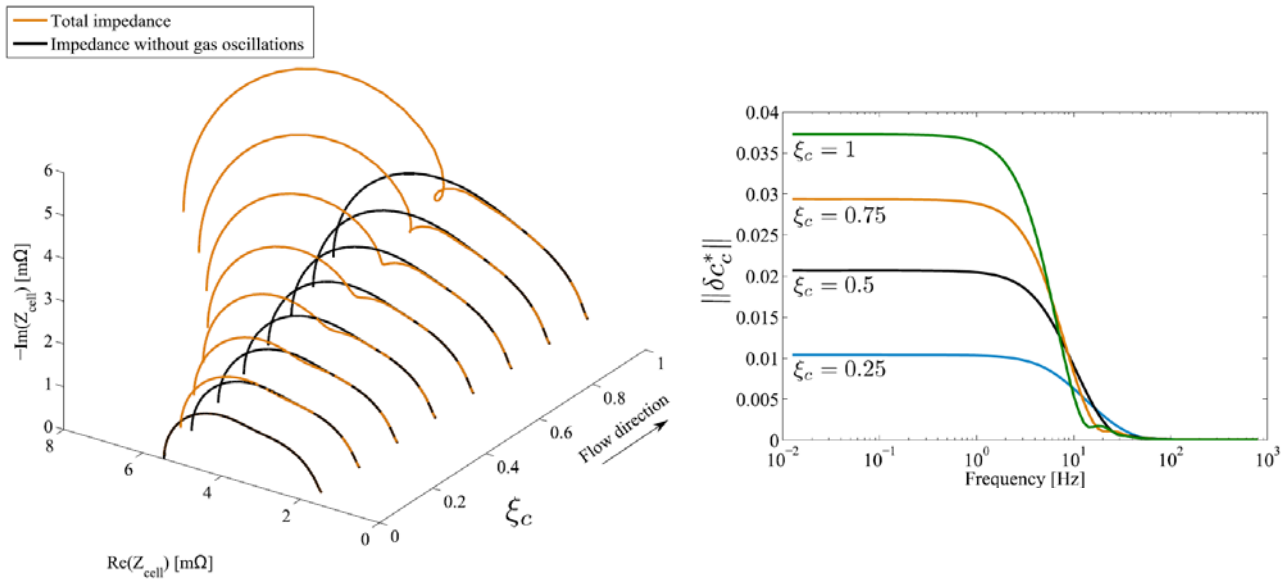

Figure 4. Local impedances along the gas channels (a) and perturbed oxygen molar concentration through the channel (b). Computed with air stoichiometry of 3.

4.2 Oxygen diffusion coefficient evaluation

The measurements presented on Figure 3 are also fitted with 1D physical model. Only the electrochemical transfers through the MEA and the GDL are solved, equations 1 to 4. Channel equations are not used. This 1D model is able to fit cell impedance with air stoichiometry of 3 in very good agreement with experimental data. Nevertheless, the oxygen diffusion obtained in this case is around 2.06 10^{-6} m²/s, three times lower than the 2D oxygen coefficient, see Table 3. With 1D model, this low oxygen diffusion is exclusively attributed to a bad oxygen transport through the GDL. Whereas 2D models had clearly shows that this loop is also link to gas oscillations. Thus, only 2D or pseudo 2D model (as this presented above) are able to identify the right oxygen coefficient value, particularly for fuel cell using parallel channels.

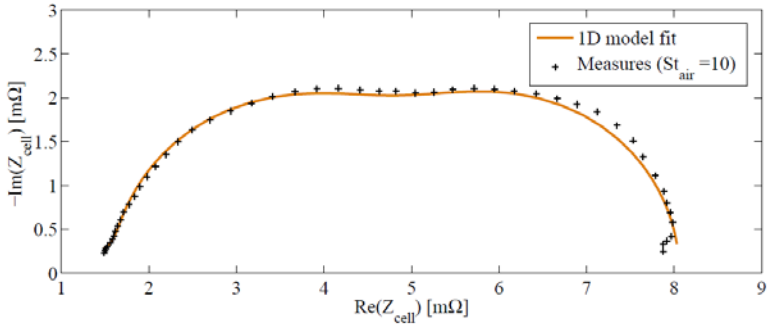

Figure 4. Local impedances along the gas channels. Computed with air stoichiometry of 3.

4. CONCLUSION

Pseudo 2D PEM fuel cell model has been built to reproduced a.c. and d.c. fuel cell behaviour. It has been able to fit on experimental impedances for several stoichiometry. Model inversion based on an hybrid criterion taking account of cell d.c. current and a.c. impedance allows more confident parameters identification. Indeed, physical cell impedance models have to be predictive on these both data.

On other hand, the main conclusion of this study is the quantification of gas channel oscillations on total impedance under classical experimental conditions : commercial fuel cells, standard stoichiometry.... It appears that this effect may be non negligible when the cell has parallel channels. Although a third loop is not clearly visible, channel impedance may interact with the gas diffusion loop in the same frequency range. This results has been confirmed by the pseudo 2D model developed above. To go further, right cell diagnosis (having parallel channels) under relative low stoichiometry conditions should be done using 2D or pseudo 2D to avoid oxygen diffusivity under-estimation.

NOMENCLATURE

η	overpotential	(V)
c	molar concentration	(mol/m^3)
i_c	exchange current	(A/m^2)
D	oxygen diffusivity	(m^2/s)
C_{DL}	double layer capacity	(F/m^2)
σ	ionic conductivity	(S/m)
E^{ref}	Nernst potential	(V)
j	cell current density	(A/m^2)
b	Tafel slope	(V)
c^{ref}	inlet channel concentration	(mol/m^3)
F	Faraday constant	(C/mol)

Subscripts

m	membrane
g	GDL
c	channel
e	electorde

REFERENCES

[1] X. Yuan, H. Wang, J. Colinsun, and J. Zhang, “AC impedance technique in PEM fuel cell diagnosis. A review,” *International Journal of Hydrogen Energy*, vol. 32, no. 17, pp. 4365–4380, Dec. 2007.

[2] J. E. B. Randles, “Kinetics of rapid electrode reactions,” *Discuss. Faraday Soc.*, vol. 1, 1947.

[3] N. Fouquet, C. Doulet, C. Nouillant, G. Dauphin-Tanguy, and B. Ould-Bouamama, “Model based PEM fuel cell state-of-health monitoring via ac impedance measurements,” *Journal of Power Sources*, vol. 159, no. 2, pp. 905–913, Sep. 2006.

[4] S. Rodat, S. Sailler, F. Druart, P.-X. Thivel, Y. Bultel, and P. Ozil, “EIS measurements in the diagnosis of the environment within a PEMFC stack,” *Journal of Applied Electrochemistry*, vol. 40, no. 5, pp. 911–920, Aug. 2009.

[5] T. E. Springer, “Characterization of Polymer Electrolyte Fuel Cells Using AC Impedance Spectroscopy,” *Journal of The Electrochemical Society*, vol. 143, no. 2, p. 587, 1996.

[6] M. Eikerling and A. . Kornyshev, “Electrochemical impedance of the cathode catalyst layer in polymer electrolyte fuel cells,” *Journal of Electroanalytical Chemistry*, vol. 475, no. 2, pp. 107–123, Oct. 1999.

[7] S. Chevalier, D. Trichet, B. Auvity, J. Olivier, C. Josset, and M. Machmoum, “PEM fuel cell impedance modelling for the detection of degraded cell parameters,” *International Journal of Hydrogen Energy*, 2013.*Accepted*.

[8] I. a. Schneider, S. a. Freunberger, D. Kramer, A. Wokaun, and G. G. Scherer, “Oscillations in Gas Channels. Part I. The Forgotten Player in Impedance Spectroscopy in PEFCs,” *Journal of The Electrochemical Society*, vol. 154, no. 4, p. B383, 2007.

[9] a. a. Kulikovsky, “A Model for Local Impedance of the Cathode Side of PEM Fuel Cell with Segmented Electrodes,” *Journal of the Electrochemical Society*, vol. 159, no. 7, Jan. 2012.

[10] G. Maranzana, J. Mainka, O. Lottin, J. Dillet, A. Lamibrac, A. Thomas, and S. Didierjean, “A proton exchange membrane fuel cell impedance model taking into account convection along the air channel: On the bias between the low frequency limit of the impedance and the slope of the polarization curve,” *Electrochimica Acta*, vol. 83, pp. 13–27, Nov. 2012.

[11] S. Chevalier, C. Josset, J. Olivier, D. Trichet, and M. Machmoum, “Experimental validation of an identification procedure of PEMFC stack state of health using EIS combined with a physical impedance modelling,”, *Chemical Engineering Transaction*, vol. 33, 2013. *Summited*